

Comparison of the toughness of different acrylonitrile-butadiene-styrene copolymers

John P. Dear*, Jan C. Graham and Paul Brown

Department of Mechanical Engineering, Imperial College of Science, Technology and Medicine, Exhibition Road, London SW7 2BX, UK

(Received 17 March 1997; revised 12 May 1997)

This study examined the change of toughness with crack velocity of two different types of acrylonitrile-butadiene-styrene (ABS) copolymers. Small laboratory specimens were used which could be precisely loaded and then allowed to stress relax before crack initiation. An experimental technique was employed which provided for good isolation of the crack initiation and propagation processes. Additionally, using this technique, it was possible to study the toughness of the materials for crack velocities from the threshold condition to the limiting crack velocity condition. © 1998 Elsevier Science Ltd. All rights reserved.

(Keywords: acrylonitrile-butadiene-styrene (ABS) copolymers; fast fracture resistance)

INTRODUCTION

Crazing, shear banding and other toughening processes at the tip of a propagating crack in polymers can be enhanced by the presence of voids or rubber particles^{1–3}. Providing the percentage volume fraction of the voids or rubber particles in the matrix material is not too large, then the other mechanical properties of the material are not greatly affected. Rubber or other second-phase particles are often preferred as toughening agents as these are easier to introduce into the matrix material and for many polymers can be more effective than voids. For example, if the rubber particles are well bonded to their host matrix, then a degree of triaxial stress will be generated in the matrix material about the rubber particle when uniaxial stress normal to the crack propagation is applied⁴. These triaxial stresses increase the propensity for crazing of the matrix material ahead of the crack tip which for some copolymers is a major toughening effect. In other copolymers, it is shear yielding of the matrix material about the rubber particles which is the more dominant toughening effect. The research interest of this study is the size and distribution of rubber particles in acrylonitrile-butadiene-styrene (ABS) copolymer that will maximize the toughening of the styrene-acrylonitrile (SAN) host matrix. Some manufacturers aim to achieve rubber particles of many different sizes, in the matrix material, whilst others prefer to have rubber particles which are more uniform in size. Of interest to many users of these ABS copolymers is how the toughness of these materials compare over a range of crack velocities from the threshold condition up to the limiting crack velocity condition. This research studied crack propagation in two types of ABS material each with the same 30% volume fraction of rubber, but with one having rubber particles of similar size and the other having rubber particles of varying size.

The frozen tongue experimental method^{5,6} was used to achieve propagating cracks in small specimens of material which could be precisely loaded normal to the intended

crack path and then allowed to stress relax before initiating a crack. Frozen tongue specimens are rectangular with a small tongue of material extending the intended crack path. ABS materials are good thermal insulators, and so it is possible to freeze cool the crack path in the tongue without reducing the temperature of the main rectangular section of the specimen. A major advantage of the frozen tongue technique is that only a small three-point bend load is required to start a sharp crack in the tongue which will propagate into the pre-loaded and stress-relaxed main section of the specimen without disturbing these loading conditions. With this technique, it is possible to produce propagating cracks, in the main section of the frozen tongue specimens, at different velocities from the threshold condition up to the limiting crack velocity condition. In this study, the required crack velocity versus load curves are obtained for the two grades of ABS and these are compared with those for the host SAN material without rubber or other toughening agents.

EXPERIMENTAL

Figure 1 shows a schematic of the three-point bend device as it is applied to the crack initiation tongue of the specimen. Specimens are often provided with a second tongue at the end of the crack path as shown in Figure 2. This second tongue provides good loading symmetry. The intended crack path was side-grooved. Cooling of the crack path in the crack initiation tongue was achieved using two metal blocks with triangular protrusions to fit into the side-grooves of the tongue. The metal blocks were cooled in liquid nitrogen and then lightly clamped into position on the tongue of the specimen. In this way, the crack path in the tongue was quickly frozen without reducing the temperature of the whole of the tongue or the main section of the specimen for more than 5 mm along the crack path. The main section of the specimen was maintained at room temperature. In addition, it was verified that when fracturing the tongue with the three-point bend device, there was negligible disturbance of the loading of the main section of

* To whom correspondence should be addressed

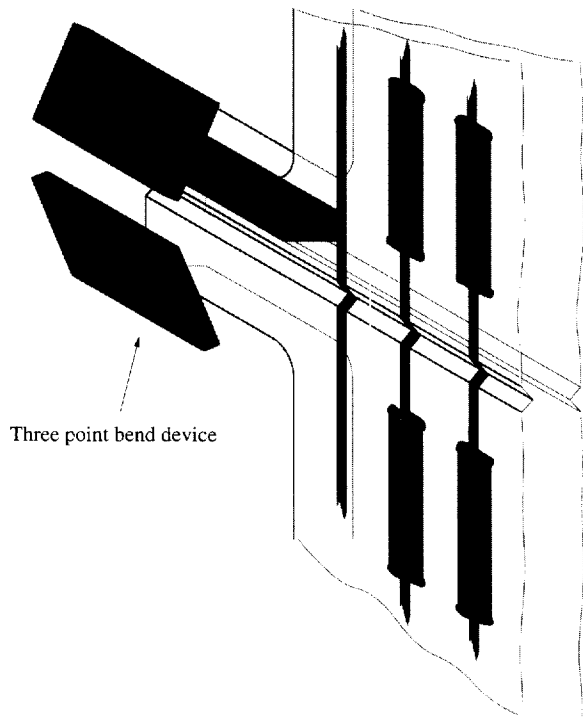


Figure 1 The three-point bend crack initiation device and its positioning on the tongue section of the specimen

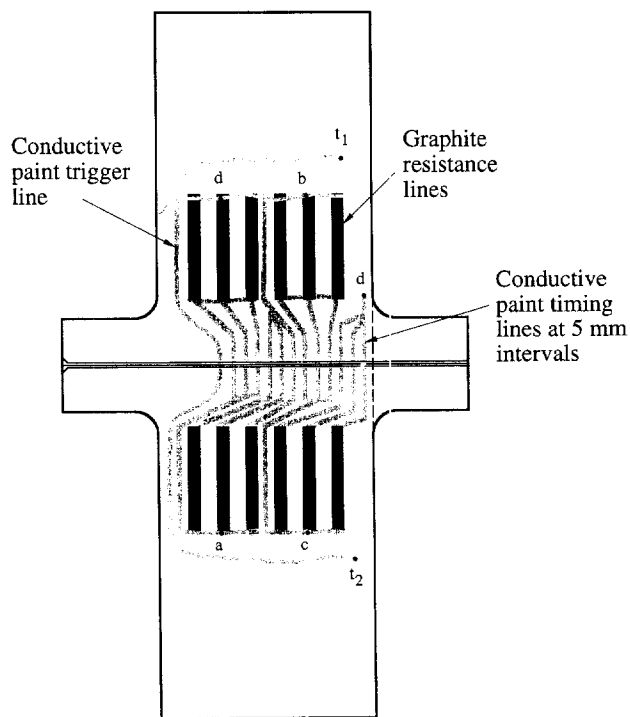


Figure 2 Frozen tongue specimen geometry. The width of the main section of the specimen is 90 mm and the full height of the main section is 300 mm and each tongue is 40 × 40 mm. The positioning of conducting strips on the frozen tongue specimen is also shown

the specimen. Another assessment made was that the disturbance of the stress field in the main section of the specimen, by the presence of the tongue, was confined to a region of 10 mm in extent from the root of the tongue.

To monitor the build-up and then constant crack velocity as the crack length in the main section of the specimen increased, a series of conducting strip monitors were located

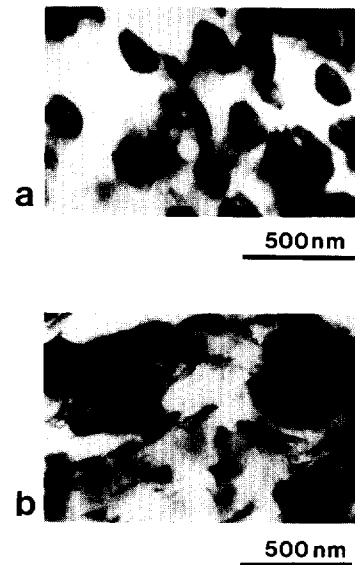


Figure 3 Transmission electron micrographs of both grades of ABS (same magnification) with rubber particles stained with osmium tetroxide: (a) ABS1; (b) ABS2

along the crack path as shown in *Figure 2*. It was found important to achieve a sharp and clean breaking of the conducting strips as the crack opened. This required the ability to form narrow conducting strips across the crack path which had to be strong enough not to be damaged when handling the specimen and mounting it in the Instron loading machine. The conducting silver paint used was manufactured by Acheson Colloids (Electrodag 915). Each strip had a graphite resistor and this was formed on the specimen using a masked spraying technique. Two separate sets of conducting strip monitoring were formed with one on each side of the specimen to obtain confirmatory outputs. The conducting strips and their graphite resistors were incorporated into a Wheatstone bridge network. As each conducting strip was broken by the propagating crack, this changed the balance of the Wheatstone bridge to produce a staircase stepping of the voltage output. These outputs from the Wheatstone bridge were monitored using a Digital Storage Scope (Gould Instrument Systems—DataSYS 740) which was equipped with facilities for transfer of the captured data to a personal computer (PC) for processing.

In addition, a completely separate monitoring of the crack tip was achieved by using a high-speed camera (Hadlands—IMACON 468). This was equipped with an optical fibre link for transfer of the photographic images to a PC. These photographic data could be correlated with those from the conducting strips.

RESULTS

Using the transmission electron microscope (TEM), thin slices of the two ABS materials were studied so as to determine the size and distribution of the rubber particles. The rubber particles were darkened by staining with osmium tetroxide. *Figure 3* shows TEM photographs of ABS1 and ABS2. *Figure 3(a)* shows ABS1 which has rubber particles of nearly the same size. *Figure 3(b)* shows ABS2 with rubber particles of variable size. It was noted in this study of particle size and their distribution in ABS2 that some of the particles gathered into closely packed groups as shown in *Figure 3(b)*.

For all the frozen tongue ABS1, ABS2 and SAN specimens, side-grooves were introduced of depth 1 mm on each side of the specimens of thickness (B) 6 mm. The load was applied to the specimens at a rate of 5 mm min^{-1} , in an Instron machine, up to the required load level and then the Instron cross-head was stopped. The specimen was allowed to stress relax before being fractured. *Figure 4* shows a loading and stress relaxation curve for an ABS1 specimen. The ABS2 and SAN specimens exhibited a similar loading and stress relaxation behaviour. After a period of time to allow the required stress relaxation, the frozen tongue technique was used to initiate a crack.

Figure 5 shows, for ABS1 specimens, the variation of crack length with time for three different stress relaxed load conditions using the conducting strip method. It can be seen that the crack upon leaving the tongue increased its velocity until full stress intensity at the crack tip was

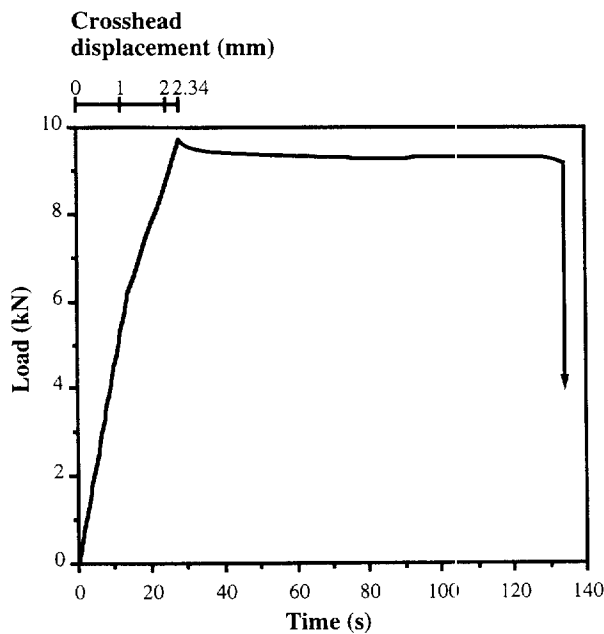


Figure 4 Load-time trace for a frozen tongue specimen of ABS1

reached when, thereafter, near to constant crack velocity was achieved. *Figure 6* shows an example of a high-speed photographic sequence of fracture in an ABS1 specimen to confirm crack velocities and other measurements made by the conducting strip method. Backlighting of the specimen was used so that the crack appeared as a bright streak of light passing through the specimen from left to right. *Figure 7* shows a comparison of the crack velocity, da/dt , versus stress relaxed load, p , for ABS1 and ABS2. *Figure 8* shows a comparison of the crack velocity, da/dt , versus stress relaxed load, p , for ABS1 and SAN. To these experimental data for ABS1, ABS2 and SAN, relationships were fitted of the form⁶:

$$(da/dt)^2 = C_L^2 \{1 - (p_0^2/p^2)\} \quad (1)$$

where C_L is the limiting crack velocity and p_0 is the threshold stress relaxed load for crack propagation.

Figure 9(a) presents the crack velocity, da/dt , versus stress relaxed load, p , for the ABS1 and ABS2 material in a different way as a plot of $(da/dt)^2$ versus $(1/p)^2$ and *Figure 9(b)* shows the same type of plot for the SAN material. These plots are useful for predicting the limiting crack velocity for the ABS materials from the experimental data. This is necessary as the ABS host material yields before conditions of high load can be reached to provide directly measurement of limiting crack velocity. This is not a problem for the SAN material when a limiting crack velocity is achieved at much lower loads. For comparison, both ABS materials (ABS1 and ABS2) and the SAN material are shown in *Figure 9*. For the reasons explained above, the limiting crack velocities for the ABS materials were obtained from extrapolation of experimental data. Hence, the 90% confidence brackets (shown as dotted lines) at the limiting crack velocity condition for ABS1 and ABS2 are wider than for the SAN material. The confidence brackets expand to give a limiting crack velocity qualified to $\pm 10\%$ for ABS1 and ABS2. However, the extrapolation is minimal for the SAN material and the limiting crack velocity is quantified to $\pm 5\%$ for SAN. *Figure 9* also shows that ABS1, ABS2 and SAN do not have a common gradient of $(da/dt)^2$ versus $(1/p)^2$ as is the case for example for different toughness grades of polyethylene⁶.

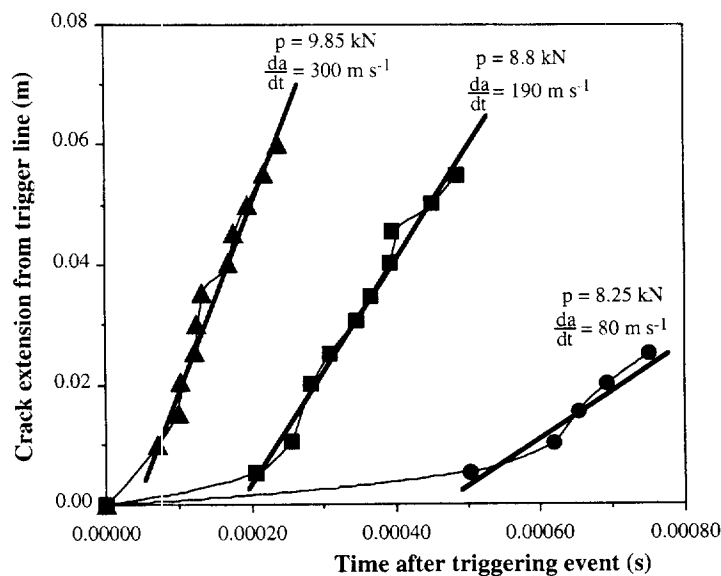


Figure 5 Crack length versus time from conducting strips for three different load conditions on ABS1 frozen tongue specimens

The toughness, R , for each of the materials evaluated, can be determined from⁶:

$$R = (\pi p_0^2) / (4EBB_n D) \quad (2)$$

where D is the specimen width, B is the overall thickness of the specimen and B_n is the crack thickness after side-grooving. The value of E used was determined by longitudinal and transverse wave velocity measurements and for an excitation frequency of 2 MHz the E -value for ABS1 was 2.7 GPa, for ABS2 it was 2.6 GPa and for SAN it was 3.3 GPa. Table 1 summarizes the fracture parameters for ABS1, ABS2 and SAN determined by the frozen tongue technique.

DISCUSSION

The presence of many well-distributed voids or rubber

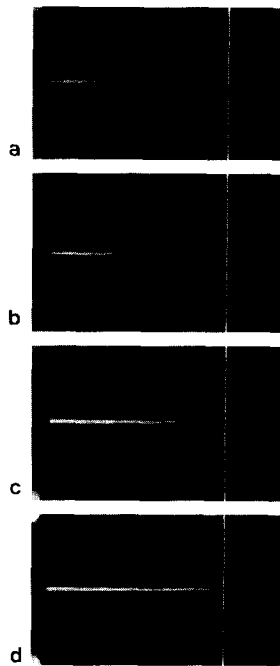


Figure 6 High-speed photographic sequence from an IMACON 468 camera of fracture of an ABS1 frozen tongue specimen

particles in a matrix material creates a multitude of stress paths through the matrix material of different cross-section. Each of these paths can have points of local stress concentration. In the case of rubber particles which are well bonded to the matrix, these rubber particles can support some stresses and in so doing produce triaxial stresses in the matrix material⁴. This can produce a notable increase of crazing and this can be a major toughening effect for some types of polymers. For ABS, the more dominant toughening effect is the increased shear yielding in the reduced cross-section of the matrix material between the rubber particles. Cavitation of the rubber particles, particularly the large ones, adds to this shear yielding process. Crack blunting and arrest by the rubber particle cavities is another factor more attributable to larger particles. These toughening effects play a large part in determining the resistance offered by ABS material to a propagating crack normal to the applied unidirectional load. However, each of these effects have different response times so that their combined effect varies with crack velocity. For example, the response time of the larger rubber particles can be greater and is one reason why it is suggested here that these have less toughening effect for higher crack velocities. Additionally, if the larger rubber particles are less effective at higher crack velocities, this results in a reduction of the volume fraction of rubber that is able to contribute to the toughness of the copolymer. However, the larger rubber particles do have an increased toughening effect at lower crack velocities, both as crack stoppers and in contributing to shear yielding, crazing and other factors. Not to be overlooked is that as the ABS material is cooled, it is deprived of the toughening effect of the rubber particles and eventually at low temperatures its toughness approaches that of the SAN material only.

For many uses of ABS, it is the increase in the threshold load and high resistance to low crack velocities which is mostly required. However, it is important to understand the behaviour of the material at higher crack velocities. This is so that the overall toughness performance of ABS and other materials can be analysed and the contribution of particle size and other factors can be assessed. Furthermore, for some applications, reducing the limiting crack velocity in addition to achieving a higher threshold load can be important requirements for structural integrity in the end-product.

Generally, there is the need in many cases to be able to

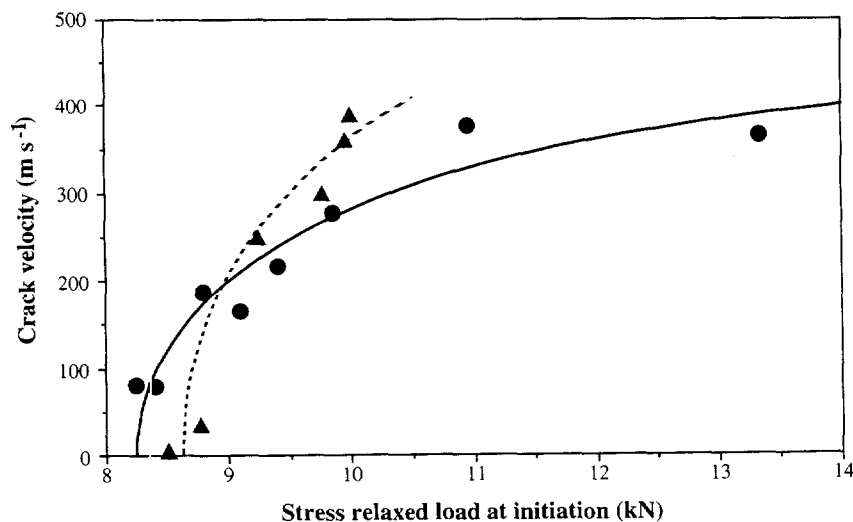


Figure 7 Crack velocity, da/dt , versus stress relaxed load, p , at crack initiation for frozen tongue experiments on ABS1 (●) and ABS2 (▲)

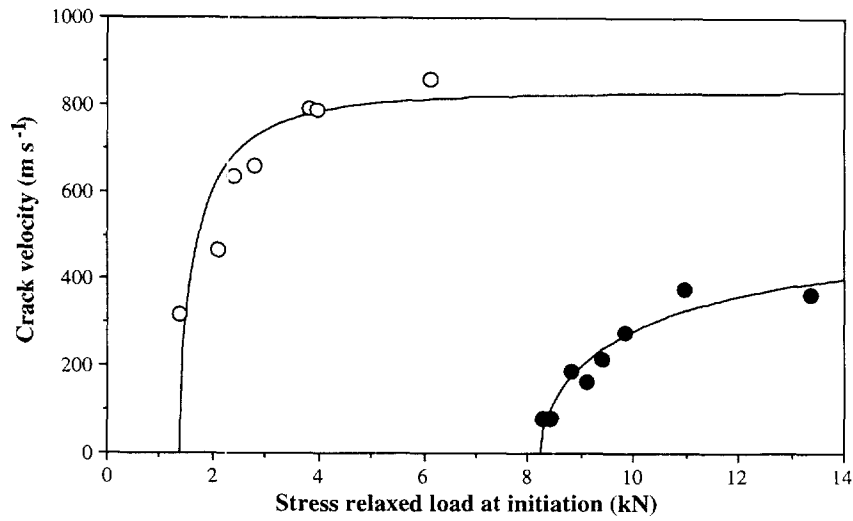


Figure 8 Crack velocity, da/dt , versus stress relaxed load, p , at crack initiation for frozen tongue experiments on ABS1 (●) and SAN (▲)

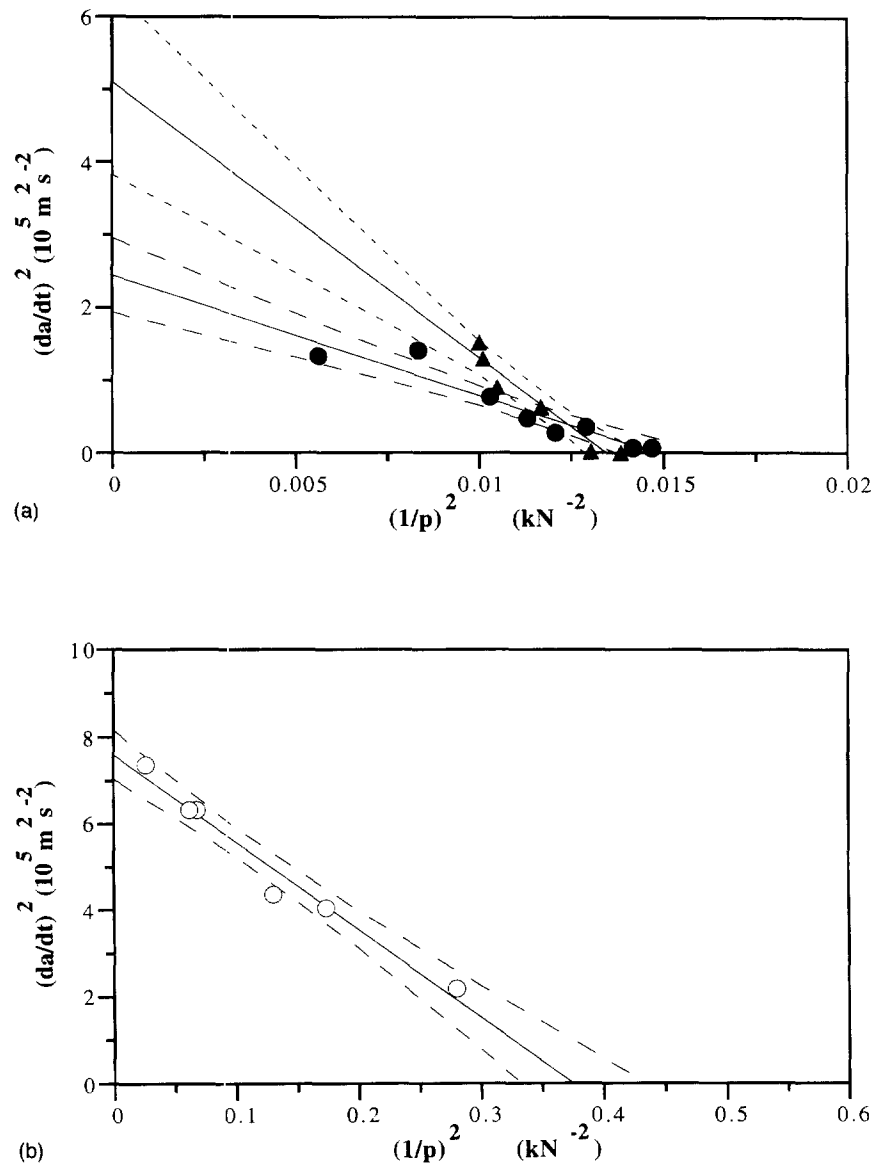


Figure 9 Plots of $(da/dt)^2$ versus $(1/p)^2$ for frozen tongue experiments on: (a) ABS1 (●) and ABS2 (▲); (b) SAN (○)

Table 1 Frozen tongue fracture parameters for ABS1, ABS2 and SAN at room temperature

Material	p_0 (kN)	C_L (m s ⁻¹)	E (GPa)	R (kJ m ⁻²)
ABS1	8.2	495 ($\pm 10\%$)	2.7	9.1
ABS2	8.6	710 ($\pm 10\%$)	2.6	10.3
SAN	1.6	870 ($\pm 5\%$)	3.3	0.3

compare the crack resistance of materials over the full velocity range from the threshold load up to the limiting crack velocity condition. For polymers which have good thermal insulation properties, the frozen tongue technique is proving to be very useful. In the case of brittle polymers, the same size and shape of frozen tongue specimens can be used but the need to cool the tongue of the specimen becomes less necessary. The result is that a very wide range of polymeric materials can be compared under precise laboratory conditions and the same experimental arrangement, so as to assess their resistance to crack propagation.

CONCLUSIONS

The results clearly show the strong toughening effect of both rubber particles of uniform size (ABS1) and those of variable size (ABS2). It was found that ABS2 offered more crack resistance than ABS1 to propagations at low crack velocities, but this advantage was lost at higher crack velocities. A notable difference between the two ABS materials is that ABS2 has some larger rubber particles which have a greater crack stopping ability at

low velocities, but are less effective at higher velocities. Not to be overlooked is that the larger rubber particles are more likely to have inclusions of matrix material which modify the dynamic response of these particles.

ACKNOWLEDGEMENTS

The authors thank the Engineering and Physical Sciences Research Council (EPSRC) and the Polymer Engineering Group (PEG) for their valuable help and support.

REFERENCES

1. Bucknall, C.B. and Smith, R.R., *Polymer*, 1965, **6**, 437.
2. Bucknall, C.B., *Advances in Polymer Science*, 1978, **27**, 121.
3. Donald, A.M. and Kramer, E.J., *Journal of Material Science*, 1982, **17**, 1765.
4. Goodier, J.N., *Transactions of the American Society of Mechanical Engineers*, 1933, **55**, 39.
5. Dear, J.P., *Journal of Material Science*, 1991, **26**, 321.
6. Dear, J.P. and Williams, J.G., *Journal of Material Science*, 1993, **28**, 259.